FEBS Letters 580 (2006) 6741–6748

ATP binding site in the plant ADP-glucose pyrophosphorylase large subunit

Seon-Kap Hwang[a], Shigeki Hamada[a,b], Thomas W. Okita[a,*]

[a] *Institute of Biological Chemistry, Washington State University, Pullman, WA 99164-6340, USA*
[b] *Division of Applied Bioscience, Graduate School of Agriculture, Hokkaido University, Sapporo 060-8589, Japan*

Received 9 October 2006; revised 12 November 2006; accepted 13 November 2006

Available online 20 November 2006

Edited by Ulf-Ingo Flügge

Abstract **The ATP binding region in the catalytically inactive large subunit (LS) of the potato tuber ADP-glucose pyrophosphorylase was identified and investigated. Mutations at the ATP binding significantly affected not only the apparent affinities for ATP and Glc-1-P, and catalytic rate but also in many instances, sensitivity to 3-phosphoglycerate. The catalytic rates of the LS mutant enzymes correlated most strongly with changes in the affinity toward ATP, a relationship substantiated by photoaffinity labeling studies with azido-ATP analog. These results indicate that the LS, although catalytically defective, interacts cooperatively with the catalytic small subunit in binding substrates and effectors and, in turn, influencing net catalysis.**

Keywords: ADP-glucose pyrophosphorylase; AGPase; ATP binding site; Enzyme kinetics; Large subunit; Photoaffinity labeling; Site-directed mutagenesis; Starch synthesis

1. Introduction

ADP-glucose pyrophosphorylase (EC 2.7.7.27; AGPase) catalyzes a pivotal, reversible reaction (glucose-1-phosphate + ATP ↔ ADP-glucose + pyrophosphate) which controls carbon flux in the starch/glycogen pathway in plants and bacteria [1–5]. AGPases from plants are heterotetrameric enzymes consisting of a pair of large subunits (LSs) and a pair of small subunits (SSs) [6,7]. Results from earlier studies using the potato (*Solanum tuberosum* L.) tuber AGPase assigned distinct roles for each subunit type: the LS was the regulatory subunit while the SS was the catalytic subunit. However, mutagenesis studies of the residues at the subunits' putative activator sites indicate that the SSs were much more important than the LS for regulation and that the main function of the LS was not to serve as an effector binding site but was required to simply modulate the regulatory properties of the SS [8,9]. In contrast to this view, analysis of subunit mosaics indicated that both subunits contributed to the regulatory properties of the heterotetrameric enzyme [10]. Moreover, our own studies on mutant enzymes containing combinations of subunits that conferred upregulatory or downregulatory properties demonstrated that the enzyme's response to effectors is a product of synergy between the LSs and SSs and not simply the LS modulating the regulatory properties of the SS [11].

The potato tuber AGPase LS appears to have little, if any, enzyme activity when co-expressed with catalytic small subunit mutants [7,12]. Mutations of residues located at or near the putative glucose-1-phosphate (Glc-1-P) binding site (K198) [13] or catalytic metal binding site (D143) [9] of the SS nearly abolished the catalytic activity. By contrast, mutations at the homologous residues of the LS only moderately affected catalysis [9]. Thus, the potato tuber AGPase LS was assumed to have no significant role in catalysis. Our recent analysis of the LS, however, showed that this subunit type is essential for optimal catalysis of the enzyme [14,15]. Interestingly, the potato tuber LS binds ATP molecules just as efficiently as the SS and mutations near the N-terminus of the LS significantly impaired the catalytic properties of the enzyme [15]. These data suggest that a specific region of the AGPase LS near the N-terminus may be a site of ATP binding.

In this study, we identified the ATP binding site of the potato tuber AGPase LS by photoaffinity labeling and mass spectrometry analysis. Juxtaposed sequence comparison and structural modeling based on the crystal structure of the homotetrameric AGPase SS [16] indicated that the reactive LS peptide is the homologous counterpart to that present in the SS ATP binding domain. Site-directed mutagenesis and subsequent kinetic analysis showed that mutations in the LS ATP binding site reduce the apparent affinity for ATP, Glc-1-P and the activator 3-phosphoglycerate (3-PGA) and catalytic properties of the heterotetrameric enzyme. Hence, although the LS lacks catalytic activity, it nevertheless participates in catalysis by affecting the capacity of the heterotetrameric enzyme to bind substrates and effectors.

2. Materials and methods

2.1. Materials

Radioactive 8-azidoadenosine 5′-[α^{32}P] triphosphate ([α^{32}P] 8-N_3ATP) and non-radioactive 8-azidoadenosine 5′-triphosphate (8-N_3ATP) were purchased from Affinity Labeling Technologies, Inc. Sodium [^{32}P] pyrophosphate and [^{14}C] glucose-1-phosphate were purchased from Perkin Elmer (NEN) and ICN Pharmaceuticals, respectively. Reagents including ATP were obtained from the Sigma-Aldrich Chemical Co. and were of analytical grade or higher.

*Corresponding author. Fax: +1 509 335 7643.
E-mail address: okita@wsu.edu (T.W. Okita).

Abbreviations: AGPase, ADP-glucose pyrophosphorylase; DTT, dithiothreitol; Glc-1-P, glucose-1-phosphate; L or LS, large subunit; PDB, Protein Data Bank; 3-PGA, 3-phosphoglycerate; S or SS, small subunit; SDS, sodium dodecyl sulfate

0014-5793/$32.00 © 2006 Published by Elsevier B.V. on behalf of the Federation of European Biochemical Societies.
doi:10.1016/j.febslet.2006.11.029

2.2. Expression and purification of the AGPase proteins

The recombinant wild-type and mutant forms of the potato tuber AGPase [7,11,17] were expressed in *Escherichia coli* EA345 cells which lack endogenous AGPase activity (*glgC* null mutation) as described in [15]. Cells were harvested and disrupted in lysis buffer (25 mM HEPES-NaOH, pH 8.0, 5% v/v glycerol) supplemented with 1 mM PMSF. Wild-type and mutant enzymes were purified according to the published procedures [15,17] with several modifications. Briefly, AGPase activity was initially fractionated on a DEAE-Sepharose Fast Flow column (Amersham) and eluted with a 0–0.5 M NaCl gradient in buffer A (25 mM HEPES-NaOH, pH 8.0, 5% glycerol). After filtration through a 1.0-μm polyethersulfone membrane (Whatman), the protein sample was purified using immobilized metal affinity chromatography (TALON™ Superflow resin, Clontech) connected to a Bio-Logic DuoFlow Chromatography system (Bio Rad). After washing with 5 mM imidazole in buffer A, the proteins were eluted with 0.15 M imidazole in buffer B (25 mM HEPES-NaOH, pH 8.0, 0.3 M NaCl, and 5% glycerol). AGPase fractions were pooled and the proteins were precipitated with pre-chilled 67% ammonium sulfate. After 2 or more hours on ice, the precipitated proteins were then carefully dissolved in 2 ml of buffer A and the solution was centrifuged at $15000 \times g$ for 10 min at 4 °C to remove denatured proteins. The enzyme solution was further diluted in 30 ml of buffer A and applied to a POROS 20HQ column (5 cm × 0.5 cm) on the FPLC system which was pre-equilibrated with buffer A. After removing contaminating proteins with 0.15 M NaCl in buffer A, the column was subjected to a 0.15–0.3 M NaCl gradient and fractions containing AGPase were pooled after SDS–PAGE analysis. After dilution with buffer A to lower the ionic strength, the enzyme solution was concentrated with ultrafiltration membrane (cutoff MW, 10 kDa; Millipore). After clarification of the enzyme solution by centrifugation, the purified enzyme preparation was aliquoted and stored at −80 °C until used for analysis.

2.3. Enzyme assay

AGPase activities were assayed in the reverse pyrophosphorylase (Assay A) direction during enzyme purification and in the forward ADP-glucose synthesis (Assay B) direction for kinetic characterization [15]. One unit (U) is defined as the amount of enzyme that produces 1 μmol of ATP or ADP-glucose for 1 min.

2.4. Labeling of AGPases with 8-azido-adenosine 5′-triphosphate

The purified AGPase was reduced in 2 mM ADP-glucose and 3 mM dithiothreitol (DTT) for 30 min at room temperature [18] and desalted into one-tenth volume of ice-cold 500 mM HEPES-NaOH (pH 7.0) using a Performa gel filtration cartridge (Edge Biosystems). Labeling reaction mixture contained 50 mM HEPES-NaOH (pH 7.0), 7 mM $MgCl_2$, 5 mM 3-PGA, and 1.2 mM of non-radioactive 8-N_3ATP for mass spectrometry analysis or varying amounts of [α-^{32}P] 8-N_3ATP (0.4 mCi/μmol) for the determination of labeling constant. Enzyme samples were exposed to 400 mJ/cm^2 of ultraviolet light for 5 min at room temperature using a UV cross-linker (Ultra-Lum, Inc., UVC-508). Immediately after UV treatment, one-half volume of the labeling stop buffer containing 150 mM HEPES-NaOH (pH 7.0), 9 mM DTT and 30% glycerol was added to stop further labeling. When needed, separation of the subunits from each other was accomplished by using a Ni-NTA column as described in [15]. The samples were then precipitated in 15% trichloroacetic acid (TCA) overnight at −20 °C to concentrate (see the following paragraph) or were directly analyzed by SDS–PAGE [17]. Autoradiography was done after drying the gel under vacuum and autoradiographic signals were quantified using the ImageJ ver.1.33 software (NIH) after scanning the X-ray films with a KODAK Electrophoresis Documentation and Analysis System 290 (EDAS 290, KODAK). Photoinsertion levels (arbitrary unit) of the 8-azidoATP analog labeling of AGPases were calculated by normalizing the labeling (photoinsertion) intensities on the film with respect to intensities of the protein bands in CBB stained gels [15].

2.5. Mass spectrometry

About 45 μg of the labeled AGPase LS protein from TCA precipitation was resolved by electrophoresis on a 8% SDS–polyacrylamide gel. After staining with Coomassie brilliant blue R-250, the labeled LS band was cut from the gel. The gel pieces were thoroughly destained with 25 mM NH_4CO_3 in 50% acetonitrile and dried under vacuum. Sixty μl of 10 μg/ml of Trypsin Gold (mass spectrometry grade, Promega) was added and the tube was placed on ice for 30 min. The tube was then placed at 37 °C for 16 h for tryptic digestion of proteins. The peptide solution was removed and dried under vacuum. The dried peptides were dissolved in 0.1% trifluoroacetic acid in water and then desalted using a ZipTipC18 tip (Millipore). The eluted peptide sample was applied to a ProteoExtract Phosphopeptide Capture Kit (Calbiochem) utilizing immobilized zirconium (IV) ions on the surface of magnetic particles to purify the phosphorylated peptides from the AGPase LS. The captured tryptic peptides were analyzed on a Voyager MALDI TOF mass spectrometer (Applied Biosystem). 2,5-Dihydroxy benzonic acid (10 mg/ml) was used as the matrix and laser power was at 2500 in a linear mode. The PeptideMass program from the ExPaSy Proteomics Server (http://ca.expasy.org/) was used to compute the masses of the generated peptides from either the LS or SS amino acid sequence.

2.6. Modeling of the ATP binding site

The three-dimensional structure of the LS ATP binding site was modeled from juxtaposed comparison with the protein sequence and crystal structure of the potato SS homotetramer [15,16]. Coordinates for the AGPase structures (1yp3 and 1yp4) were obtained from RCSB Protein Data Bank (PDB) (http://www.rcsb.org/pdb/). DeepView, the Swiss-PdbViewer (http://www.expasy.org/spdbv/), was used for modeling and Pov-Ray (http://www.povray.org/) was used for rendering the structure.

2.7. Site-directed mutagenesis

Oligonucleotide primers used in this study are listed in Table 1. Ten nanogram of the plasmid DNA harboring either the AGPase large subunit or small subunit sequence [15] was used as the template for mutagenesis. The QuikChange site-directed mutagenesis kit (Stratagene) was used to introduce the mutation. PCR conditions were 16 cycles at 95 °C for 30 s, 56 °C for 1 min, and 68 °C for 14 min. *E. coli* XL10-Gold™ (Stratagene) was used for selection of mutants as well as subsequent cloning and propagation of the plasmids. DNA sequencing with the ABI 3100 automated capillary sequencer (Applied Biosystems) was performed to verify the entire sequences of the LS and SS for the desired mutations. The LS and SS sequences were then transferred to protein expression plasmids, pSH274 and pSH208, respectively [15]. The various cell lines were analyzed for glycogen production by culturing them on NZCYM agar media containing 100 mg/l ampicillin and 50 mg/l kanamycin, and 0.4% v/v glycerol as a carbon source which readily allows the efficiently induced expression of both subunits from the *lac*/*tac* dual promoter [15]. pBAD99A plasmid (4.0-kb) was constructed using *Nco*I and *Nde*I restriction enzymes to replace the *tac* promoter and $lacI^Q$ region (1.7-kb) of pTrc99A [19] with the *BAD* promoter and *araC* regulator region (1.6-kb) of pBAD-TOPO (Invitrogen). The LS sequences cloned on the pSH274 were then transferred to this plasmid by cloning using *Nco*I/ and *Sac*I restriction enzymes. The resulting plasmids were transformed into EA345 cells containing pSH228. NZCYM agar medium containing 0.01% L-arabinose (Sigma), 100 mg/l ampicillin, and 50 mg/l kanamycin was used for growing cells to assess glycogen production.

2.8. Determination of kinetic and labeling constants

Kinetic parameters of AGPases were determined in the ADP-glucose synthesis direction as described in [11,15]. One unit (U) of enzyme activity is defined as 1 μmol of ATP or ADP-glucose produced for 1 min at 37 °C. The kinetic values ($S_{0.5}$, $A_{0.5}$, k_{cat}, and $k_{cat}/S_{0.5}$) and labeling constant (K_L) were determined using the modified Hill equations [20] in Kaleidagraph (Synergy software) as described in [15].

2.9. Protein analysis

Measurements of protein concentration and SDS–PAGE were performed as described in [17].

Table 1
Oligonucleotide primers used in this study

Mutation	Direction	Sequence
G36A	Sense	5′-GCTGCAGTCATACTGGGA**GCA**GGAGAAGGGACCAAGTTA-3′
	Antisense	5′-TAACTTGGTCCCTTCTCC**TGC**TCCCAGTATGACTGCAGC-3′
G37A	Sense	5′-GCAGTCATACTGGGAGGA**GCA**GAAGGGACCAAGTTATTC-3′
	Antisense	5′-GAATAACTTGGTCCCTTC**TGC**TCCTCCCAGTATGACTGC-3′
K41R	Sense	5′-GGAGGAGGAGAAGGGACC**CGT**TTATTCCCACTTACAAGT-3′
	Antisense	5′-ACTTGTAAGTGGGAATAA**ACG**GGTCCCTTCTCCTCCTCC-3′
T51K	Sense	5′-CTTACAAGTAGAACTGCA**AAA**CCTGCTGTTCCGGTTGGA-3′
	Antisense	5′-TCCAACCGGAACAGCAGG**TTT**TGCAGTTCTACTTGTAAG-3′
Q127M	Sense	5′-GAAGCAGGAAAAAAATGGTTT**ATG**GGAACAGCAGATGCTG-3′
	Antisense	5′-CAGCATCTGCTGTTCC**CAT**AAACCATTTTTTTCCTGCTTC-3′
G128A	Sense	5′-GCAGGAAAAAAATGGTTTCAA**GCA**ACAGCAGATGCTGTTA-3′
	Antisense	5′-TAACAGCATCTGCTGT**TGC**TTGAAACCATTTTTTTCCTGC-3′
G128L	Sense	5′-GCAGGAAAAAAATGGTTTCAA**CTG**ACAGCAGATGCTGTTA-3′
	Antisense	5′-TAACAGCATCTGCTGT**CAG**TTGAAACCATTTTTTTCCTGC-3′
T129V	Sense	5′-GGAAAAAAATGGTTTCAAGGA**GTG**GCAGATGCTGTTAGAA-3′
	Antisense	5′-TTCTAACAGCATCTGC**CAC**TCCTTGAAACCATTTTTTTCC-3′
A132V	Sense	5′-TTTCAAGGAACAGCAGAT**GTT**GTTAGAAAATTTATATGG-3′
	Antisense	5′-CCATATAAATTTTCTAAC**AAC**ATCTGCTGTTCCTTGAAA-3′
A132F	Sense	5′-TTTCAAGGAACAGCAGAT**TTT**GTTAGAAAATTTATATGG-3′
	Antisense	5′-CCATATAAATTTTCTAAC**AAA**ATCTGCTGTTCCTTGAAA-3′
A132D	Sense	5′-TTTCAAGGAACAGCAGAT**GAT**GTTAGAAAATTTATATGG-3′
	Antisense	5′-CCATATAAATTTTCTAAC**ATC**ATCTGCTGTTCCTTGAAA-3′
A132N	Sense	5′-TTTCAAGGAACAGCAGAT**AAT**GTTAGAAAATTTATATGG-3′
	Antisense	5′-CCATATAAATTTTCTAAC**ATT**ATCTGCTGTTCCTTGAAA-3′
T129V/A132V	Sense	5′-TTTCAAGGAGTG**GTG**GCAGAT**GTT**GTTAGAAAATTTATATGG-3′
	Antisense	5′-CCATATAAATTTTCTAAC**AAC**ATCTGC**CAC**TCCTTGAAA-3′
D157L	Sense	5′-ATCGTTGTACTATCTGGG**CTG**CATCTTTATAGGATGGAT-3′
	Antisense	5′-ATCCATCCTATAAAGATG**CAG**CCCAGATAGTACAACGAT-3′
D157N	Sense	5′-ATCGTTGTACTATCTGGG**AAT**CATCTTTATAGGATGGAT-3′
	Antisense	5′-ATCCATCCTATAAAGATG**ATT**CCCAGATAGTACAACGAT-3′
D157E	Sense	5′-ATCGTTGTACTATCTGGG**GAA**CATCTTTATAGGATGGAT-3′
	Antisense	5′-ATCCATCCTATAAAGATG**TTC**CCCAGATAGTACAACGAT-3′
G267L	Sense	5′-CCCACTTCTAATGATTTT**CTG**TCTGAAATTATACCAGCA-3′
	Antisense	5′-TGCTGGTATAATTTCAGA**CAG**AAAATCATTAGAAGTGGG-3′
G267S	Sense	5′-CCCACTTCTAATGATTTT**AGC**TCTGAAATTATACCAGCA-3′
	Antisense	5′-TGCTGGTATAATTTCAGA**GCT**AAAATCATTAGAAGTGGG-3′
D143N (SS)	Sense	5′-TACCTTATACTTGCTGGA**AAC**CATCTGTATCGAATGGAT-3′
	Antisense	5′-ATCCATTCGATACAGATG**GTT**TCCAGCAAGTATAAGGTA-3′
LSPP2		5′-CAGCATTCCTGTCAATATGGTTCTGCA-3′
PLS-2		5′-GCTTATCATCGATAAGCTTCCTTCGG-3′
Trc99-F		5′-TAATCATCCGGCTCGTATAATGTGTG-3′
LSPCR-S2		5′-GCTAGCTTGGCACTCACACAAGAGT-3′
M13-47		5′-CGCCAGGGTTTTCCCAGTCACGAC-3′
QE34		5′-CGGATAACAATTTCACACAG-3′
LSPCR-S	Sense	5′-CTTGAAATGGAGCTATCCCACTTCT-3′
LSPCR-AS	Antisense	5′-CACAATCTAAGCGCGATCTTTCA-3′

$D_{143}N$ sense and antisense primers were used for generating a mutation on the small subunit of the potato tuber AGPase.
The codons for mutation are shown in boldface.

3. Results and discussion

3.1. Identification of ATP binding domain in the large subunit

We had previously demonstrated that 8-N_3ATP was a near equivalent substitute for the substrate ATP in the catalytic reaction of AGPase [15]. Under photoaffinity labeling conditions, the analog bound to both AGPase subunits with equal efficiency rendering the enzyme catalytically inactive. To identify the adenine binding domain for ATP in the putative non-catalytic LS, the 8-N_3ATP labeled subunit was subjected to trypsin digestion and the nucleotide-bound peptides were isolated. Mass spectrometric analysis of labeled (Fig. 1A) and unlabeled (Fig. 1B) samples showed two prominent unique peaks (M_r = 1592.89 Da and M_r = 1512.69 Da) present in only the 8-N_3ATP-labeled sample. Taking into account the acid lability of the terminal phosphate ester bond [21], the peaks at M_r = 1592.89 Da and M_r = 1512.69 Da correspond to ADP- and AMP-bound ^{125}WFQGTADAVR^{134} from the LS, respectively. This reactive peptide from the LS is homologous to a peptide located in the ATP binding site of the catalytic SS. Moreover, structural modeling of the LS (Fig. 2A and B) based on the crystal structure of the potato SS homotetramer (PDB 1yp3) [16] supports the role of this peptide in ATP binding. Specifically, residues Q127, G128, T129, and A132 contained within the reactive peptide W125-R134 of the LS are predicted to interact directly or indirectly with the adenine moiety of ATP. The carbonyl group and side chain of Q127 and the carbonyl group of G128 form hydrogen bonds with adenine N6. The side chain of T129 participates in interaction with the γ-phosphate group of ATP, while its carbonyl group forms a hydrogen bond with the main-chain nitrogen of A132. In addition, these modeling studies predict G36 and G37

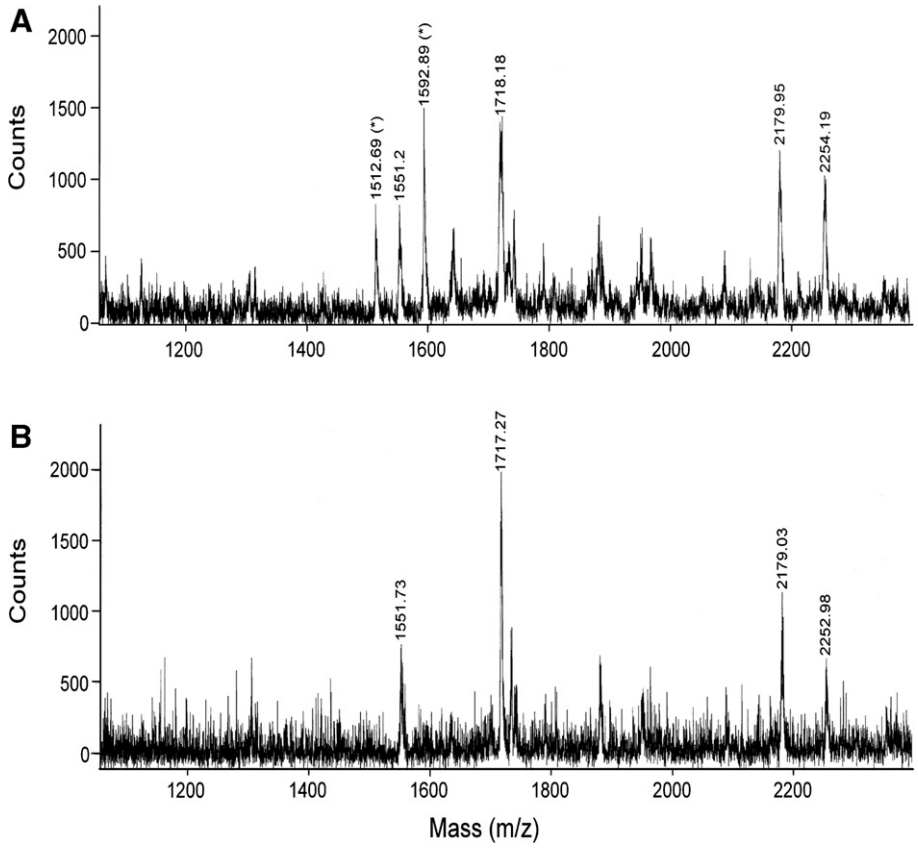

Fig. 1. Mass spectrometric analysis of the ATP binding region in the AGPase large subunit. Tryptic digests of the AGPase LS labeled with 8-N_3ATP (A) and non-labeled LS as a control (B) were subjected to a MALDI TOF mass spectrometry. Two peaks with molecular masses of 1512.69 Da and 1592.89 Da were identified and indicated with asterisks. *m*/*z*, mass-to-charge ratio.

residues of the glycine-rich P-loop as well as G267 and D157, interacting with the adenine ring of ATP. Although, a previous study [9] suggested that D157 in the LS was not important for catalysis of AGPase, the residue is still predicted to be associated with a ribose moiety of ATP in our model. Main chain nitrogen of G267 together with the side chain of T129 is expected to interact with γ-phosphate moiety of ATP.

3.2. Generation of the ATP-binding site mutants

Selected residues predicted to participate in ATP binding as described above were replaced with amino acids with different side-groups by site-directed mutagenesis using the respective primers listed in Table 1. K41 and T51 were also selected for analysis because mutations at these residues were able to resurrect catalytic activity of the LS when assembled with catalytically inactive SS_{D143N} [12]. In addition, the crystal structure of the AGPase homotetramer bound with ADP-glucose (PDB 1yp4) reveals that the side chains of these equivalent residues in the SS (R31 and K41) form hydrogen bonds with β-phosphate and ribose moiety of the substrate, respectively [16].

The various mutant LSs were co-expressed with wild-type SSs in EA345 cells [15] grown on glycerol-containing agar media or on L-arabinose-containing agar media. The catalytic activities of these mutant enzymes were initially assessed by their capacity to restore glycogen production as viewed by iodine staining. Compared to wild-type cells, lines expressing the various mutant enzymes showed varying capacity to accumulate glycogen ranging from normal to null staining (Fig. 2C and D). On glycerol media, G36A and Q127M showed wild-type levels of glycogen, while G37A, T51K, and T129V accumulated intermediate levels. By contrast, G128A, A132V and D157L showed no discernible glycogen staining, indicating that these residues are important for enzyme activity. When the AGPase mutants were expressed under the BAD promoter on arabinose media, a slightly different profile pattern of glycogen accumulation was obtained (Fig. 2D). While the iodine staining phenotype of G36A and Q127M mutants was unaltered showing similar levels of glycogen accumulation to wild-type, G37A and T51K showed much lower capacity to accumulate glycogen while T129V was essentially a null phenotype under these growth conditions. This lower capacity to accumulate glycogen by these various AGPase mutant lines is likely due to the weaker expression by the BAD promoter than by the *lac*/*tac* dual promoter and different composition of culture media. In fact, when the green fluorescence protein was used as a reporter gene, the *lac*/*tac* promoter produced more proteins than the BAD promoter (result not shown).

3.3. Kinetic properties of the wild-type and mutant enzymes

We purified the mutant enzymes to near homogeneity (>95% of purity) and carried out enzymatic analysis to characterize their kinetic properties. Overall, the kinetic properties of the various mutant enzymes were in keeping with their capacity to direct glycogen accumulation in the various mutant lines. G36 and Q127 had no obvious effects on the apparent k_{cat} values, while G128A, A132V, and D157L led to significantly low-

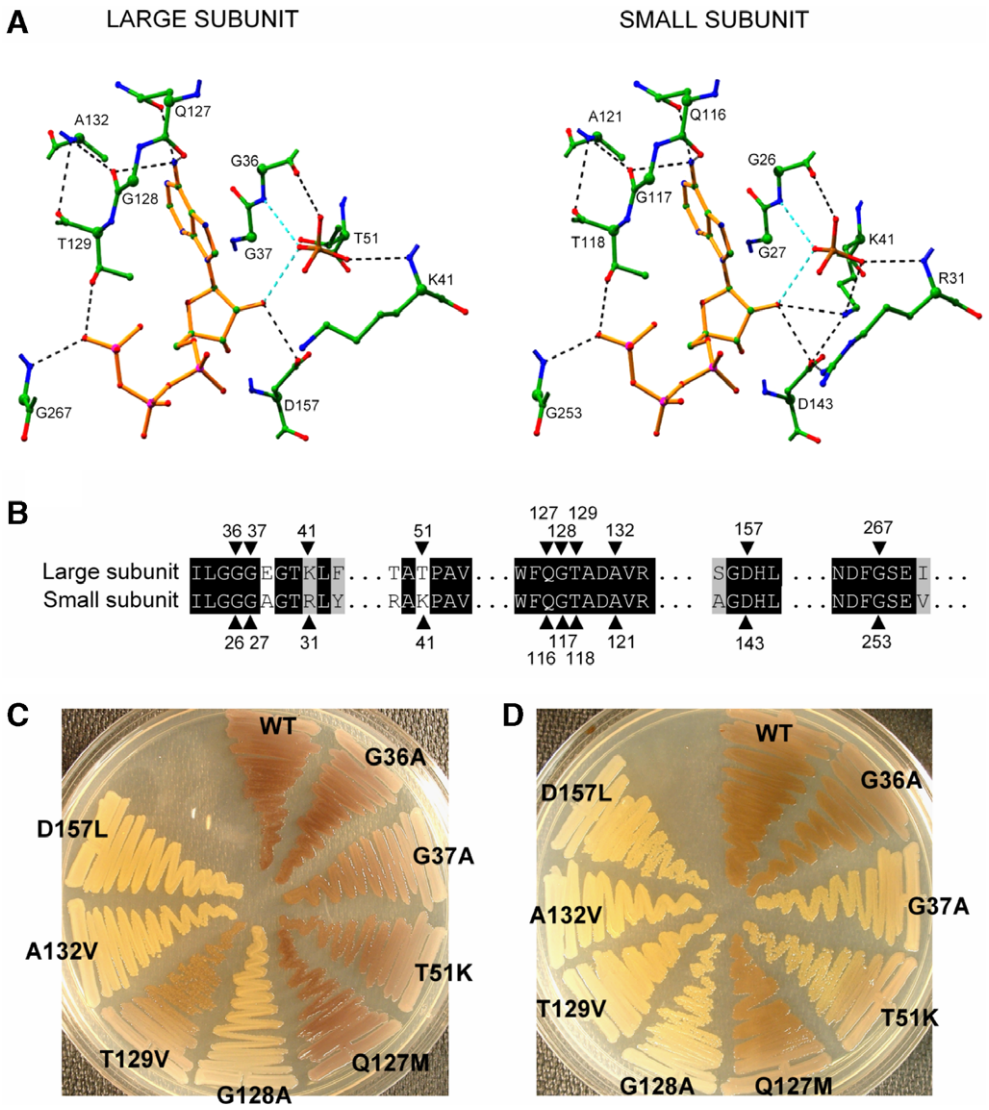

Fig. 2. ATP binding residues in the large and small subunits of AGPase. (A) The ATP binding sites of the large and small subunits were modeled. The structure of ATP is shown in orange. Carbon is shown in green, nitrogen in blue, oxygen in red, sulfur in brown, and phosphorus in pink. (B) Homology comparison of the ATP binding residues of the AGPase large and small subunits. Residue numbers are indicated above or below the subunit sequences. Iodine staining of the *E. coli* EA345 cells co-expressing the wild-type (WT) SS with various LSs under the control of *lac*/*tac* promoter (C) and *BAD* promoter (D) (see Section 2).

ered (5–11-fold) catalytic rates compared to wild-type, while the remaining residues show intermediate levels of catalytic activity. The apparent affinity values toward ATP were only moderately affected by the mutations (about 2-fold). Interestingly, the enzyme's affinity towards Glc-1-P was more severely compromised by these specific mutations: 4.4-fold for G128A, 5.4-fold for T129V, and 8.1-fold for A132V. When catalytic efficiency was considered, the effects of the mutations were more pronounced (10–22-fold). The more significant impact of these mutations on the apparent binding constants for Glc 1-P rather than for ATP is consistent with the sequential ordered *bi*/*bi* kinetic mechanism proposed for AGPase catalysis. As ATP binds first followed by Glc 1-P, alteration of the bound ATP is likely to have a more pronounced effect on subsequent binding of Glc 1-P.

Further mutations at G128, A132, D157, and G267 also greatly lowered catalytic activities (up to 10-fold) depending on the type of the substituted amino acid (Table 2). As expected, the double mutant $L_{T129V/A132V}S_{WT}$ showed pronounced decreases in the substrate affinities (2.5-fold for ATP) and catalytic rates (20-fold) (Table 2) compared to wild-type.

Interestingly, except for the K41R mutations, all of the mutations resulted in decreased apparent affinity to the activator 3-PGA (Table 3) with substitutions at G36, G37, T51, T129, A132, and D157 having the most effect. As the ATP and effector binding sites are in close proximity [16], these results indicate that the integrity of the ATP binding domain of the LS is also important for the effector binding site and, in turn, the net regulatory properties of the enzyme. Interestingly, the T51K mutation gave rise to reduced catalytic properties as well as decreased sensitivity to 3-PGA (Tables 2 and 3). Although the impaired catalytic properties of this enzyme are consistent with the intermediate iodine staining and reduction in glycogen levels (Fig. 2D), they were unexpected based on previous results on the restoration of the catalytic activity

Table 2
Catalytic properties of the AGPase wild-type and mutants

Subunit		ATP				Glc-1-P			
Large	Small	$S_{0.5}$ (mM)	*n*H	k_{cat} (s^{-1})	CE (s^{-1} M^{-1})	$S_{0.5}$ (mM)	*n*H	k_{cat} (s^{-1})	CE (s^{-1} M^{-1})
WT	WT	0.17	1.5	166	975	0.10	1.1	158	1585
G36A	WT	0.26	1.5	142	547	0.40	0.9	133	332
G37A	WT	0.24	1.3	43	179	0.25	1.0	40	158
K41R	WT	0.19	1.4	139	732	0.24	1.5	145	602
T51K	WT	0.24	1.6	85	352	0.32	1.0	93	290
K41R/T51K	WT	0.27	1.5	83	308	0.22	1.3	81	370
Q127M	WT	0.18	1.7	143	796	0.16	1.5	154	963
G128A	WT	0.36	1.5	33	93	0.44	1.0	33	75
G128L	WT	0.46	1.2	12	27	0.71	1.0	11	15
T129V	WT	0.30	1.5	45	150	0.54	0.8	47	87
A132V	WT	0.36	1.3	16	44	0.81	0.7	23	29
A132D	WT	0.39	1.3	18	45	0.64	1.0	16	25
A132N	WT	0.39	1.2	22	57	0.63	0.9	21	34
A132F	WT	0.35	1.2	19	56	0.97	0.8	24	25
D157L	WT	0.40	1.4	15	38	0.22	1.0	15	70
D157N	WT	0.58	1.4	75	130	0.12	1.2	63	526
D157E	WT	0.32	1.2	43	133	0.15	1.2	33	223
G267L	WT	0.57	1.4	23	41	0.47	0.9	27	57
G267S	WT	0.21	1.4	107	512	0.16	1.4	98	612
T129V/A132V	WT	0.43	1.3	8	17	0.88	1.2	10	23
WT	D143N	0.31	1.6	0.03	0.1	ND	ND	0.03	ND
D157L	D143N	ND	ND	0.003	ND	ND	ND	0.002	ND
K41R	D143N	0.40	1.6	0.07	0.18	0.38	1.0	0.07	0.2
T51K	D143N	0.43	1.2	4.1	10	1.01	1.0	4	10
K41R/T51K	D143N	0.35	1.1	11.9	34	0.17	1.6	9	34

All values were determined from ADP-glucose synthesis assay data of at least two iterations, and the standard errors (SEs) were less than 15% in all cases. Only the mean values are presented here. The apparent $S_{0.5}$ and k_{cat} values for ATP and Glc-1-P were obtained under the saturating condition where 10 mM of 3-PGA was added. *n*H, Hill coefficient; CE, catalytic efficiency; $k_{cat}/S_{0.5}$ (s^{-1} M^{-1}), $\times 10^3$; ND, not determined.

Table 3
3-PGA sensitivity of the wild-type and mutant AGPases

Subunit		3-PGA		
Large	Small	$A_{0.5}$ (mM)	*n*H	Specific activity (U/mg)
WT	WT	0.12	0.9	42.0
G36A	WT	0.65	1.0	40.5
G37A	WT	0.79	1.0	9.5
K41R	WT	0.12	0.8	37.5
T51K	WT	0.72	1.0	23.7
K41R/T51K	WT	0.53	0.9	23
Q127M	WT	0.25	0.9	39.8
G128A	WT	0.41	0.9	7.6
G128L	WT	0.51	1.1	3.2
T129V	WT	1.24	1.0	14.2
A132V	WT	0.90	0.8	5.4
A132D	WT	0.49	1.0	5.6
A132N	WT	0.62	1.1	6.7
A132F	WT	0.70	0.9	5.2
D157L	WT	1.28	1.0	5.2
D157N	WT	1.17	1.0	19.1
D157E	WT	1.38	1.0	13.4
G267L	WT	0.74	0.9	6.5
G267S	WT	0.24	1.0	26.8
T129V/A132V	WT	0.96	0.9	1.6
WT	D143N	0.30	0.6	0.01
D157L	D143N	ND	ND	ND
K41R	D143N	0.03	0.8	0.02
T51K	D143N	0.04	0.7	1.02
K41R/T51K	D143N	0.04	0.8	2.9

All values were determined in the ADP-glucose synthesis direction (see Section 2). At least two iterations were done and the mean values are presented here. The standard errors (SEs) were <15% in all cases. The $A_{0.5}$ for 3-PGA was obtained under the saturating substrate conditions where 1.5 mM ATP and 2 mM Glc-1-P were added. *n*H, Hill coefficient; ND, not determined.

of the LS [12]. When combined with the catalytic defective S_{D143N}, the $L_{T51K}S_{D143N}$ had 54-fold higher catalytic activity than $L_{WT}S_{D143N}$. Thus, the catalytic-enabled L_{T51K} interacts adversely with the more powerful catalytic S_{WT}, resulting in a reduction in the net catalytic properties of the heterotetrameric enzyme.

3.4. Relationship between substrate/activator affinity and catalytic activity

Since introduction of many of the ATP binding mutations in the LS affected catalytic, substrate affinity and regulatory properties of the enzyme (Tables 2 and 3), we wanted to know which kinetic property was the most important in affecting the catalytic rate (activity). We determined the relationships between the different kinetic properties (apparent $S_{0.5}$ for ATP and Glc-1-P and $A_{0.5}$ for 3-PGA) and catalytic rates (k_{cat}) of the wild-type and mutant AGPases (Fig. 3). All of the relationships (*r* values) examined in this study were statistically significant ($r > r_{critical} = 0.575$ at $P = 0.01$). Of the various parameters examined, the strongest relationship was evident between the catalytic rate and apparent $S_{0.5\ ATP}$ values ($r = 0.95$) with lesser values obtained for Glc-1-P ($r = 0.67$), both substrates ($r = 0.8$), and 3-PGA ($r = 0.74$). Although the apparent affinities for ATP were not severely altered by these mutations, these results indicate that the predicted ATP binding residues in the LS are, nevertheless, closely associated with net catalytic activity.

3.5. Photoaffinity labeling of the large subunit mutant

The double mutant $L_{T129V/A132V}S_{WT}$ showed impaired catalytic properties (Table 2). In order to determine whether the

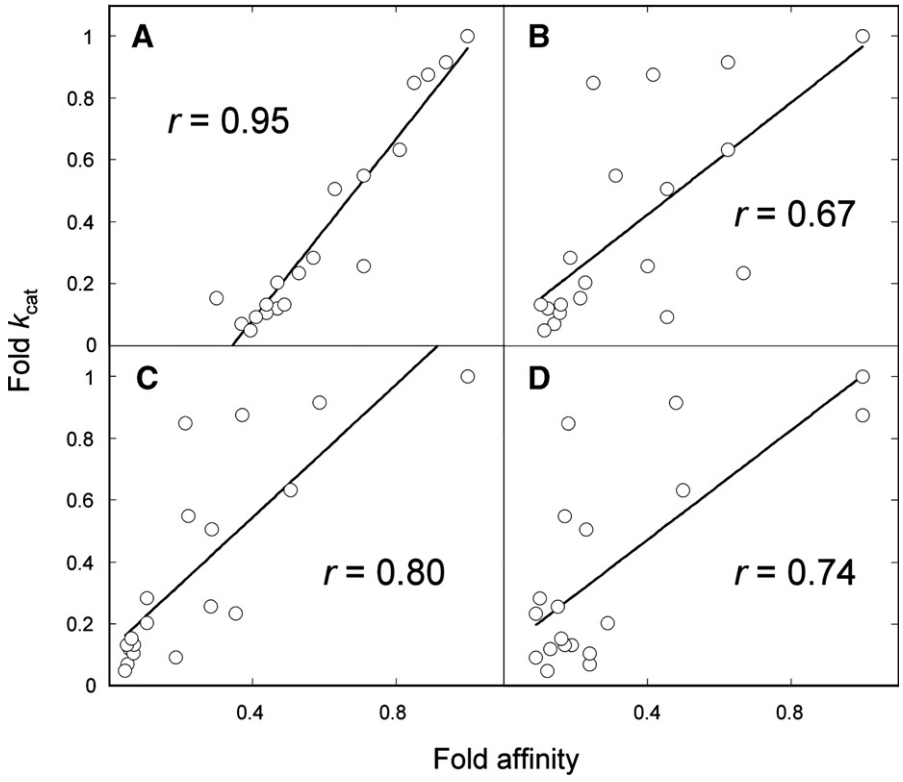

Fig. 3. Relationship between substrate/activator affinities and catalytic rates of the mutant AGPase LSs. Fold $k_{cat} = k_{cat}$(mutant)/k_{cat} (wild-type). Fold affinity was calculated by (A) $S_{0.5,ATP\,(wild\text{-}type)}/S_{0.5,ATP\,(mutant)}$, (B) $S_{0.5,Glc\text{-}1\text{-}P\,(wild\text{-}type)}/S_{0.5,Glc\text{-}1\text{-}P\,(mutant)}$, (C) A × B, and (D) $A_{0.5,3\text{-}PGA\,(wild\text{-}type)}/A_{0.5,3\text{-}PGA\,(mutant)}$. r, correlation (Pearson) coefficient (critical coefficient, r_{crit}, is 0.575 at $P = 0.01$).

mutation also affected ATP binding per se, we photo-affinity labeled the double mutant and wild-type AGPase enzymes with various concentrations of [α^{32}P] 8-N_3ATP in the absence of Glc-1-P. Fig. 4 shows that $L_{T129V/A132V}S_{WT}$ was less efficiently labeled than the wild-type. When the degree of photoaffinity labeling (photoinsertion) versus concentration of the analog was plotted using a modified Hill equation, the determined half-maximal saturation concentration (K_L value) of the wild-type was 0.18 mM and that of the mutant was 0.40 mM. These values are nearly identical to the apparent $S_{0.5ATP}$ values (0.17 mM for wild-type and 0.43 mM for the double mutant) obtained by kinetic analysis (Table 2). These results indicate that the T129 and A132 in the LS are important for ATP binding and enzyme's catalysis. Thus, the LS plays an important role in enzyme catalysis.

It has been suggested that the SS plays a dominant role over the LS in the enzyme catalysis and the LS is a modulatory subunit since the LS has no or very little catalytic activity [9,12,13]. Indeed, the catalytic activity of $L_{WT}S_{D143N}$ is decreased by more than four orders of magnitude compared

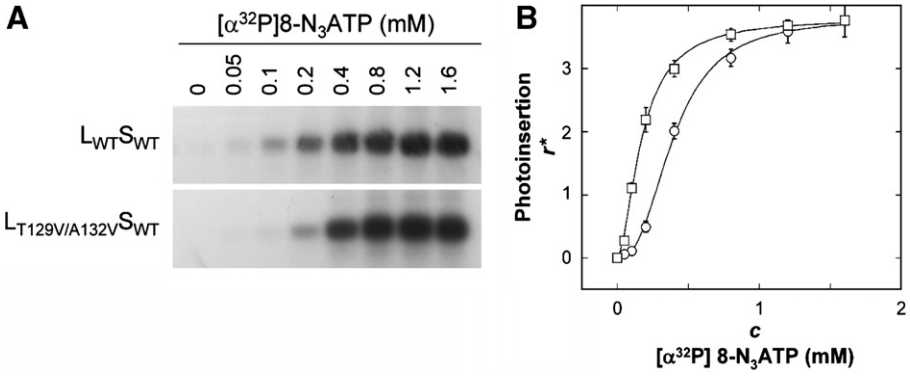

Fig. 4. Photoaffinity labeling of the wild-type and LS double mutant. (A) Wild-type ($L_{WT}S_{WT}$) and LS double mutant ($L_{T129V/A132V}S_{WT}$) AGPases (1.5 μg each) were labeled with varying amounts (0–1.6 mM) of [α^{32}P] 8-N_3ATP and then separated by electrophoresis on 10% SDS–polyacrylamide gels. The polyacrylamide gel was stained with CBB R-250, dried, and autoradiographed. (B) The extent of [α^{32}P] 8-N_3ATP incorporation of the wild-type (open squares) and T129V/A132V double mutant (open circles) AGPases. The labeling curve was plotted using the modified Hill equation [$r^* = (R^*_{max}c^h)/(K^h_L + c^h)$]. r^* represents the normalized photoinsertion by dividing the labeling intensities of the protein bands on the X-ray film with the intensities of the protein bands on CBB stained gel, R^*_{max} the maximal photoinsertion, c the concentration of [α^{32}P] 8-N_3ATP, h Hill coefficient, and K_L the equilibrium binding (labeling) constant.

to wild-type [9], an observation confirmed in this study (Table 2). The mutation at K198 (putative Glc-1-P binding site) of the SS also led to a drastic loss of catalytic activity [13].

Nonetheless, several lines of evidence indicate that the LS is more directly involved in enzyme catalysis than simply modulating the properties of the catalytic SS. First, the contemporary LS, which has evolved from the SS still retains very high sequence and structural homology to the SS [12,15]. The LS binds ATP as efficiently as the SS [15] as well as ADP-glucose [13]. Moreover, the catalytic activity of the LS can be resurrected by two amino acid substitutions near the ATP binding pocket. Second, in addition to mutations at the ATP binding site of the LS that directly affect the enzyme's catalytic activity (this study; Table 2, Figs. 3 and 4), mutations at P44 of the LS significantly reduced the catalytic activities and substrate specificities of AGPase [15]. Structurally, P44 is situated only two amino acids away from the glycine-rich putative ATP binding site which encompasses amino acids 35–42 in the same loop structure of the LS. Since major structural changes were not evident from circular dichroism data, the mutation at P44 may cause subtle but effective changes in local structure of the LS which disturb the spatial orientation of bound ATP in the LS. Collectively, although the SS contains the active catalytic site, these results strongly implicate the involvement of the LS in specifying the catalytic properties of the AGPase heterotetrameric enzyme.

The exact molecular basis for the involvement of the LS in catalysis of the heterotetrameric AGPase is not known. However, a likely mechanism is inferred from results from an earlier study [11], which demonstrated that the regulatory properties of the enzyme are a product of synergy between the LS and SS. In this same light, the LS and SS interact cooperatively in binding substrates with the LS undergoing a 'pseudo-catalytic' cycle in conjunction with the catalytic activity of the SS. In support of this view, Jin et al. [16] have shown that the A/A′ (SS counterpart) and B/B′ (the potential LS counterpart) subunits of the homotetrameric enzyme undergo large structural changes upon binding of ATP [16]. Thus, the substrate binding properties of the LS, the functional equivalent of the B-type subunit of the homotetrameric enzyme, may impact the substrate binding properties of the SS and, in turn, catalytic properties of the enzyme.

Acknowledgement: This work was supported by DoE Grant No. DE-FG02-96ER20216 and falls under the purview of the Hatch Regional NC-1142 Project.

References

[1] Preiss, J. (1984) Bacterial glycogen synthesis and its regulation. Annu. Rev. Microbiol. 38, 419–458.
[2] Slattery, C.J., Kavakli, I.H. and Okita, T.W. (2000) Engineering starch for increased quantity and quality. Trends Plant Sci. 5, 291–298.
[3] Ballicora, M.A., Iglesias, A.A. and Preiss, J. (2004) ADP-glucose pyrophosphorylase: a regulatory enzyme for plant starch synthesis. Photosynth. Res. 79, 1–24.
[4] Kleczkowski, L.A. (2000) Is leaf ADP-glucose pyrophosphorylase an allosteric enzyme. Biochim. Biophys. Acta 1476, 103–108.
[5] Tiessen, A., Hendriks, J.H., Stitt, M., Branscheid, A., Gibon, Y., Farre, E.M. and Geigenberger, P. (2002) Starch synthesis in potato tubers is regulated by post-translational redox modification of ADP-glucose pyrophosphorylase: a novel regulatory mechanism linking starch synthesis to the sucrose supply. Plant Cell 14, 2191–2213.
[6] Okita, T.W., Nakata, P.A., Anderson, J.M., Sowokinos, J., Morell, M. and Preiss, J. (1990) The subunit structure of potato tuber ADPglucose pyrophosphorylase. Plant. Physiol. 93, 785–790.
[7] Iglesias, A.A. et al. (1993) Expression of the potato tuber ADP-glucose pyrophosphorylase in *Escherichia coli*. J. Biol. Chem. 268, 1081–1086.
[8] Ballicora, M.A., Fu, Y., Nesbitt, N.M. and Preiss, J. (1998) ADP-glucose pyrophosphorylase from potato tubers. Site-directed mutagenesis studies of the regulatory sites. Plant Physiol. 118, 265–274.
[9] Frueauf, J.B., Ballicora, M.A. and Preiss, J. (2003) ADP-glucose pyrophosphorylase from potato tuber: site-directed mutagenesis of homologous aspartic acid residues in the small and large subunits. Plant J. 33, 503–511.
[10] Cross, J.M., Clancy, M., Shaw, J.R., Greene, T.W., Schmidt, R.R., Okita, T.W. and Hannah, L.C. (2004) Both subunits of ADP-glucose pyrophosphorylase are regulatory. Plant Physiol. 135, 137–144.
[11] Hwang, S.K., Salamone, P.R. and Okita, T.W. (2005) Allosteric regulation of the higher plant ADP-glucose pyrophosphorylase is a product of synergy between the two subunits. FEBS Lett. 579, 983–990.
[12] Ballicora, M.A., Dubay, J.R., Devillers, C.H. and Preiss, J. (2005) Resurrecting the ancestral enzymatic role of a modulatory subunit. J. Biol. Chem. 280, 10189–10195.
[13] Fu, Y., Ballicora, M.A. and Preiss, J. (1998) Mutagenesis of the glucose-1-phosphate-binding site of potato tuber ADP-glucose pyrophosphorylase. Plant Physiol. 117, 989–996.
[14] Kavakli, I.H., Greene, T.W., Salamone, P.R., Choi, S.B. and Okita, T.W. (2001) Investigation of subunit function in ADP-glucose pyrophosphorylase. Biochem. Biophys. Res. Commun. 281, 783–787.
[15] Hwang, S.K., Hamada, S. and Okita, T.W. (2006) The catalytic implications of the large subunits of the higher plant ADP-glucose pyrophosphorylase. Phytochemistry, in press, doi:10.1016/j.phytochem.2006.11.027.
[16] Jin, X., Ballicora, M.A., Preiss, J. and Geiger, J.H. (2005) Crystal structure of potato tuber ADP-glucose pyrophosphorylase. EMBO J. 24, 694–704.
[17] Hwang, S.K., Salamone, P.R., Kavakli, H., Slattery, C.J. and Okita, T.W. (2004) Rapid purification of the potato ADP-glucose pyrophosphorylase by polyhistidine-mediated chromatography. Protein Expr. Purif. 38, 99–107.
[18] Fu, Y., Ballicora, M.A., Leykam, J.F. and Preiss, J. (1998) Mechanism of reductive activation of potato tuber ADP-glucose pyrophosphorylase. J. Biol. Chem. 273, 25045–25052.
[19] Amann, E., Ochs, B. and Abel, K.J. (1988) Tightly regulated tac promoter vectors useful for the expression of unfused and fused proteins in Escherichia coli. Gene 69, 301–315.
[20] Bell, J.E. and Bell, E.T. (1988) Proteins and Enzymes, Prentice-Hall, Inc., Englewood Cliffs, NJ, pp. 465–470.
[21] Wolff, R. and Paysant, P. (1951) Hydrolysis of ATP by trichloracetic acid. Bull. Soc. Chim. Biol. (Paris) 33, 1871–1876.